Engineering and Technology Journal
Journal homepage: https://etj.uotechnology.edu.iq

Deposition of GdSmTi Coating for Corrosion Control of *SS 316L* in Bio-Field

Shaimaa A. Naser , Rana A. Anaee* , Hussein A. Jaber

Materials Engineering Dept., University of Technology-Iraq, Alsina'a street, 10066 Baghdad, Iraq.
*Corresponding author Email: Dr.rana_afif@yahoo.com

HIGHLIGHTS

- GdSm-Ti coating enhances stainless steel's corrosion resistance, achieving a protection efficiency of 99.02%.
- The dense compact layer formed by GdSm-Ti coating reduces surface roughness and improves wettability.
- Coated stainless steel shows excellent corrosion protection and enhanced osteointegration.

ARTICLE INFO

Handling editor: Akram R. Jabur

Keywords:
Samarium
Gadolinium
Titanium
Coating
Bioimplant
Sputtering

ABSTRACT

The corporation of rare earth metals (lanthanides series) with other metals gives good properties in different fields, such as protecting the metallic surface from corrosion risk. In this work, the investigation on adding gadolinium (Gd) and samarium (Sm) as rare metals to bio-inert titanium (Ti) as transition metal was done to protect stainless steel (SS 316L) as bio metallic implant which is used in biofield because of its excellent mechanical properties, low costs, biocompatibility, inertness, and mechanical properties, chemical stability, workability, and high corrosion resistance. The corporation was done through coating using direct current (DC) sputtering technique from the target of these metals mixture to measure some properties. The surface characterization by X-ray diffraction (XRD) gave many phases represented by different Gd_xNi_y in addition to the Ni_3Ti phase and Ni_5Sm phase. The scanning electron microscopy and energy dispersive X-ray spectroscopy (SEM/EDS) results showed the distribution of coating metals as a dense thin film with a good ratio of coating metals; this dense film gave lower surface roughness as illustrated through Atomic force microscopy (AFM) examination from 25.20 nm for the uncoated sample to 15.12 nm for the coated sample with a reduction in the hardness from 187 HV for the uncoated sample to 119 HV for the coated sample as well as increasing contact angle test (wettability) from 90° for base stainless steel surface to 117.723° for coated surface, these results enhanced the compatibility with giving good resistance from corrosion test, with achieving protection efficiency equal to 99.02%.

1. Introduction

The coating is an attempt to cover the metallic surface with a protective layer to act as a physical barrier between a material and the environment and to limit the electrochemical processes and get long-term protection. The applied coatings must achieve an aesthetic appearance, protection from damage, and specific attributes to the product. Therefore, a huge variety of materials were present to use as a coating that was applied by different techniques to support the requirements of the application in addition to providing some suitable properties such as hardness, softness, antimicrobial and anti-corrosion, etc. The used coating metals in this work are represented by Ti from the transition metals that are referred to as the d block elements including groups (3-12) of the periodic table with different oxidation states in their compounds and have been used in medicinal biochemistry [1,2], titanium is used in different ways in bio applications like (bone fixation, hip joint, etc.) because it has good mechanical properties like low elastic modulus and high strength, abrasion resistance, and low density due to the low hardness; also biological properties represented by strong chemical stability and biocompatibility, as well as being inert and having good resistance to corrosion. On the other hand, the rare-earth metals (Lanthanides) that include the f block elements from lanthanum to lutetium exhibit a pronounced biological activity, and they have unique positions in a periodic table with interesting properties in a variety of biochemical reactions and they are used as structural and functional probes in understanding structures, conformations, and properties of biomolecules, in general, these metals have trivalent oxidation states [3], such as samarium which is utilized in promoting antibacterial activity, osteoblastic performance low toxicity and an adequate safety profile, previous research has shown Sm^{3+}containing materials have superior antimicrobial properties. Also,

http://doi.org/10.30684/etj.2023.138741.1404
Received 06 March 2023; Accepted 15 May 2023; Available online 20 June 2023
2412-0758/University of Technology-Iraq, Baghdad, Iraq

gadolinium has antibacterial properties and excellent anticorrosion performance. Furthermore, Gd is used as a drug carrier and anticancer agent, and its presence of Gd promote osteoconductivity and cell growth. Improving biological and anti-corrosion properties is made possible by gadolinium. Gadolinium is highly stable in the human organ's environment [4]. These two rare earth metals (Sm and Gd) were added to Ti in the coating mixture.

Many techniques were used to apply coatings, such as direct electrocathodic deposition, pulse electrocathodic deposition, chemical vapor deposition, physical vapor deposition, electrophoretic deposition, magnetron sputtering, plasma spray deposition, pulsed laser deposition, and sol−gel coatings. The coating by direct current DC sputtering using transition Ti metal was applied, where binary Ti– Nb coatings by co-sputtering from Ti and Nb metallic targets were deposited by Achache et al. [5], tantalum-titanium oxynitride TaTiON thin films were deposited by Daniel et al. [6], using DC sputtering in a mixture of nitrogen/oxygen ratio (85%/15%), the properties of Ta_2O_5 monolayer, Ta_2O_5/Ti bilayer and $Ta_2O_5/Ta_2O_5 - Ti/Ti$ multilayer coatings on the $Ti - 6Al - 4V$ alloy were estimated by Zeliang et al. [7], including the adhesion strength, tribological behaviors, corrosion resistance and mechanical properties using DC sputtering, while $Pt - Ti$ coatings and characterize an intermetallic Pt_3Ti layer were studied by Pascal et al. [8], using co-sputtering from metallic Pt and Ti targets in pure Ar atmosphere.

Many mixtures were applied as coating with rare-earth metals, where a thin film of TiO_2 and $(Nd_yTi_{1-y})O_x$ was deposited by Michal et al. [9], $(Ca_{10-x}Sm_x(PO_4)_6(OH)_2$ was applied by Simona et al. [10], using RF sputtering. On the other hand, gadolinium oxide Gd_2O_3 was deposited by Saranya et al. [11], using electrophoretic deposition on anodized Mg alloy, and Gd conversion coating was applied also by Saranya et al. [12], on a biodegradable AZ31 Mg implant, samarium oxide Sm_2O_3 was deposited by Saranya et al. [13], on AZ31 Mg alloy in the biofield, antibacterial coatings of hydroxyapatite HA nanoparticles doped Sm with two different concentrations were deposited by Ionela et al. [14], using the dip coating method.

In the current work, $Gd - Sm$ with Ti was deposited on SS 316L by DC sputtering technique, and then the characterization and measure some properties for the coated surfaces were done.

2. Materials and Methods

2.1 Materials

SS 316L specimens were used to apply GdSmTi coating; these specimens had a chemical composition done in Centralized Device for Standardization and Quality Control-Ministry of Planning (0.03 C, 0.03 P, 0.75 Si, 1.50 Mn, 0.01 S, 3.00 Mo, 16.00 Cr, 12.00 Ni, 0.05 N wt% and Fe remain). The grinding method with SiC papers in the series of $(400,600,800,1000,1200,\text{and } 2000$ grain sizes) and polishing with Al_2O_3 paste was achieved on square specimens $(15\times15\times3$ mm) to get the mirror finishing surface, because of exist any dust or dirt on the surface specimen before the coating that considers as an extra layer between the coating material and sample surface, this extra layer obstructs the coating process and prevent adhesion of the coating material on the sample surface.

2.2 Coating process

Sputtering that provided to enhance adhesion between coating and substrate with a decreased thickness of the deposited coating layer, the chance of cracking and coating failure decreases. Significantly enhances coating adhesion offers a less porous microstructure and reinforces its bonding strength for a long period.

The applied DC sputtering on SS 316L surfaces was done with a disk of (stainless steel) and plasma source under some experimental conditions, as listed in Table 1. All coating materials were in the purity of 99%; where Ti was from Fluka chemical AGCH-9470 Buckes, Switzerland, with particle size 165 μm, $Gd(NO_3)_3.6H_2O$ and $Sm(NO_3)_3.6H_2O$ were from Glentham Life Science Company, UK) that used with a ration of $(30\text{wt\%}Gd(NO_3)_3.6H_2O - 30\text{wt\% }Sm(NO_3)_3.6H_2O -$ 40wt% pure Ti) in a target with dimensions of (diameter 50 mm and thickness 5 mm).

Table 1: Conditions of DC sputtering process

DC power supply	Deposition time	Work pressure	Initial pressure	Voltage	Electrical current	Gas atmosphere
4 kV	3 h	4×10^{-2}mmbar	1×10^{-4} mmbar	1500 V	25 mA	Ar

2.3 Characterization Methods

Many methods were used to characterize the coated surfaces, including X-ray diffraction XRD (Shimadzo, 6000) at room temperature to identify the formed phases at a scanning speed of $5/\text{min}$ using Cu Kα radiation (λ=1.5405 A°), with an applied power (40 KV and 30 mA), scanning electron microscope (SEM) (FEIQUANTA 250, Czech Republic) to show the particles shape and calculate the thickness and Atomic Force Microscope (AFM) (NaioAFM 2022 nanosufr, Switzerland, and ultrasharp gold tip) to investigate the topography and surface roughness.

2.4 Corrosion Measurement

The electrochemical properties were estimated by recording an open circuit potential scan (OCP) for one hour, linear and cyclic polarization scan using three electrodes (Saturated Calomel electrode (SCE) as a reference, Pt electrode as counter, and $SS\ 316L$ samples as working) in Ringer Lactate medium obtained from (Pharmaceutical Solution Industry) after adjusting pH

by sodium bicarbonate ($NaHCO_3$) to 7.4 value. All tests were carried out using Compactstat (Potentiostat/ galvanostat), and Ivium under controlled software at 37°C, and the data was measured using the Tafel extrapolation method.

2.5 Hardness

The microhardness was recorded for uncoated and coated specimens using an indenter by Digital Microhardness (HMV-2, Shimadzu, Kyoto, Japan) under a load of 300 gm and a holding time of 15 sec.

2.6 Wettability

This test was done using the sessile drop device consisting of a tube electrical resistance furnace (for the sessile drop on the substrate), camera, furnace, and outer mulite tube with a diameter of (50mm), an internal diameter of (30mm) and length of (270mm) and internal mulite tube with outer diameter of (25mm) and internal diameter of (20mm) and length of (275mm).

3. Results and Discussion

3.1 Characterization of Coated Surface

3.1.1 XRD analysis

The phases present after coating can be seen as a mixture of main intermetallic phases such as Ni_3Ti, Ni_5Sm, and Gd_2Ni_{15} despite of there being no Ni in the target but can get from the substrate. The Ti tends to form titanium oxide TiO_2 rather than/or before to produce any phase with Sm and Gd. On the other hand, Gd tends to form many intermetallic comds with Ni, including GdNi, $GdNi_2$, $GdNi_3$, Gd_2Ni_7, $GdNi_5$ and Gd_2Ni_{17} that are associated with various invariant reactions and have the electric and magnetic hyperfine interactions [15], the XRD of the GdSmTi coated specimen is shown in Figure 1.

In the study of Guanglong et al. [16], they showed that the microstructure of a two-phase for Gd_3Ni in equilibrium with GdNi occurs rather than Gd_3Ni_2. In another study for the phase stability of the Rare Earth-Transition Metal (RE−TM) compounds, it was observed that the formation of RE_3TM_2 and $RETM_4$ generally takes place in the RE−Ni systems with rare earth found at the right side of Gd in the periodic table, (i.e., Tb or Dy), but not with a RE on the left of Gd (i.e., Sm and Eu). The fact that the RE − Ni system is like the "dividing line" in the presence of the compound system.

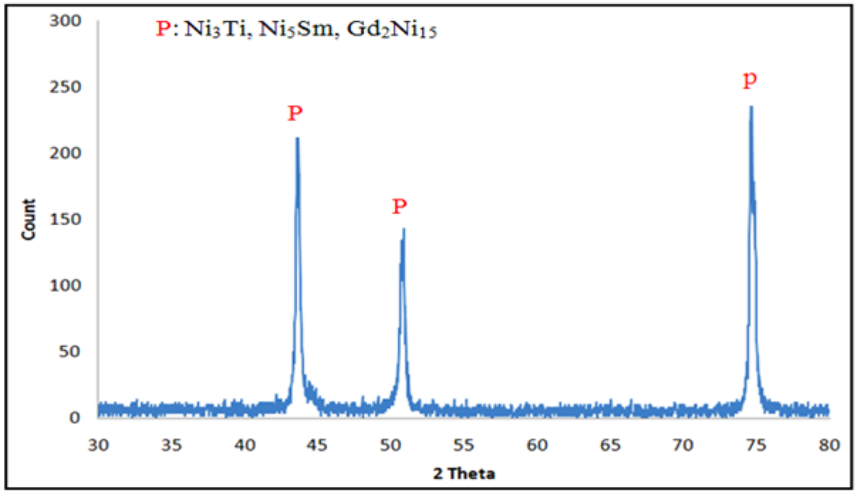

Figure 1: XRD pattern of $GdSmTi$ coated SS $316L$

3.1.2 SEM/EDS analysis

The microstructure of the GdSmTi coated specimen in Figure 2 (a) shows the compact dense layer for the phases of Gd and Sm with Ni closed to a substrate covered by TiO_2 layer that gave the feature like to that observed for preparation of inactive TiO_2, also indicate that few porosity and little scratch on the coated surface as anatase and rutile that showed by Drushan et al. [17]. The complete image of the EDS analysis in Figure 2 (b) gave the main elements of stainless steel 316L (substrate), including Fe, Ni, Cr, C and Mo, as well as the distribution of the coating elements as Gd, Sm and Ti with wt% of 16.2, 21.2 and 11.7 % respectively. This also confirms the formation of the main intermetallic compound such as Ni_3Ti, Ni_5Sm, and Gd_2Ni_{15}. The weight percent of RE is higher than Ti, confirming the incorporation role for RE phases with TiO_2 in protection.

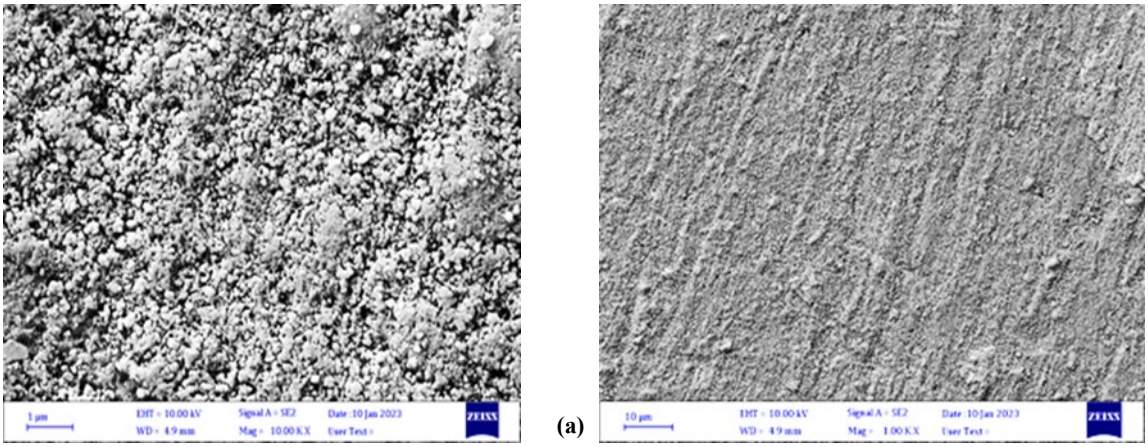

(a)

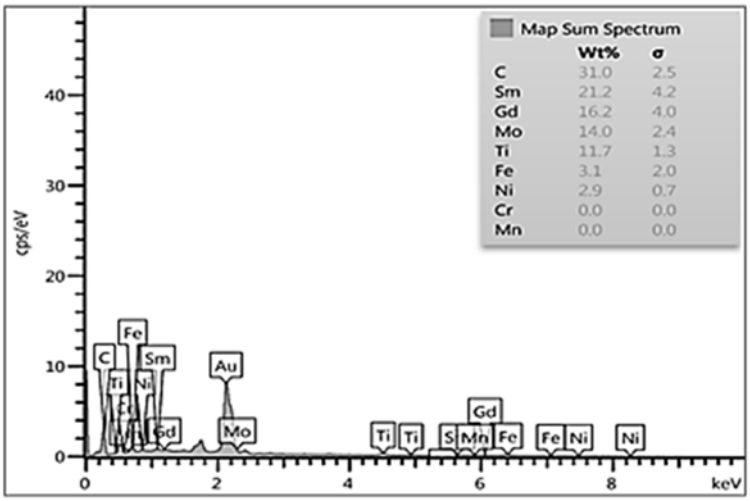

(b)

Figure 2: (a) SEM of $GdSmTi$ coated $SS\ 316L$ (b)SEM/EDS of $GdSmTi$ coated $SS\ 316L$

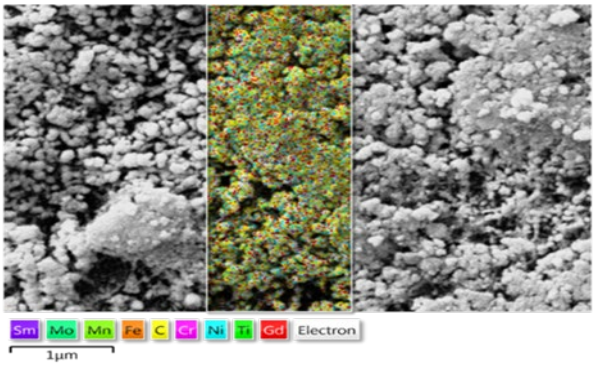

(a)

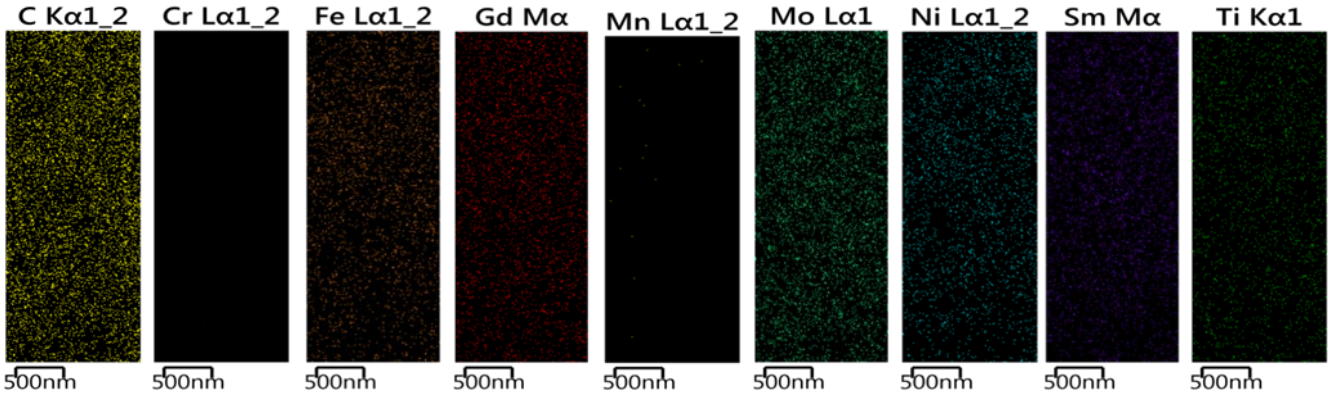

(b)

Figure 3: (a,b) Mapping of $GdSmTi$ coated $SS\ 316L$

The mapping figure for $GdSmTi$ coating gave the different metals indicating the presence of these metals in the coating layer and achieved clear information on the main content elements (Fe, Cr, Ni, Ti and Sm). The distribution of coating metals as thin film and metals in the substrate can be seen by mapping analysis in Figure 3 (a,b). Also, the compact layer of coating can be observed by the cross-section figure for coated specimen, where the coating is distinguished from the bulk. The cross-sectional analysis illustrated that the coating is characterized by a thin film with a particle size in the range of 17.86 – 35.73 nm, i.e., deposition of a thin film in a nanometer scale, as shown in Figure 4 (a,b,c) at different magnifications.

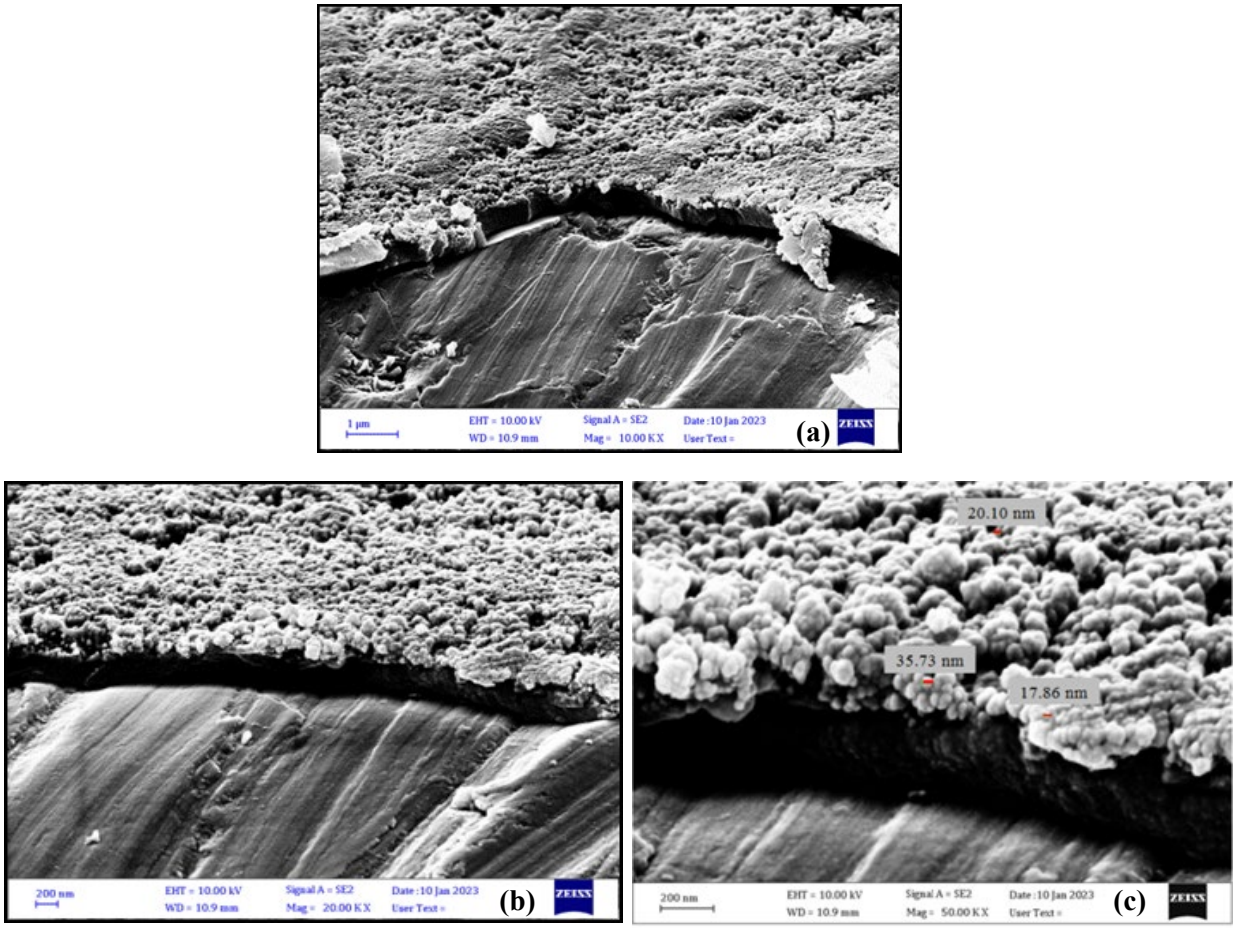

Figure 4: Cross section of $GdSmTi$ coated $SS\ 316L$

3.1.3 AFM Analysis

AFM examination shows the 2D and 3D images of the morphology of the films for coated and uncoated surfaces, indicating the dense layer of the current coating due to the Gd metal and displaying a preferred orientation; this is consistent with the different XRD phases as shown in Figure 5 (a,b). There is a clear reduction in all parameters estimated from AFM examination, especially in the maximum height and depth, where they reached half value (125.7 → 62.37 nm) and (81.84 → 47.7nm) respectively due to the dense compact uniform deposited layer and finally, it gave lower surface roughness to be 15.12nm. The reduction in roughness was also observed by Shalini et al. [18], who created Sm_2O_3 films on fused quartz and Si substrates and they indicated that the reduction in roughness from AFM analysis is attributed to the growth of grains and simultaneous nucleation of both the cubic and monoclinic phases that making the deposited film less faceted and smoother.

The particle analysis of coated surface Figure 6 (a,b) confirms the getting dense compact layer of the coating through the decreasing in main diameters from (710.8nm) to (119nm) and increasing the number of particles from 123 to 603 after coating as well as the increase in the density from 1,254,502 to 14,873,792 $Particle/mm^2$ due to the dense compact layer of coating with coverage by 46.51%.

Table 2: AFM data of uncoated and coated specimens

Parameter	Uncoated (nm)	Coated (nm)
Root-mean-square height (S_q)	32.08	20.39
Maximum peak height (S_p)	125.7	62.37
Maximum pit depth (S_v)	81.84	47.70
Maximum height (S_z)	207.5	110.1
Arithmetic mean height (S_a)	25.20	15.12

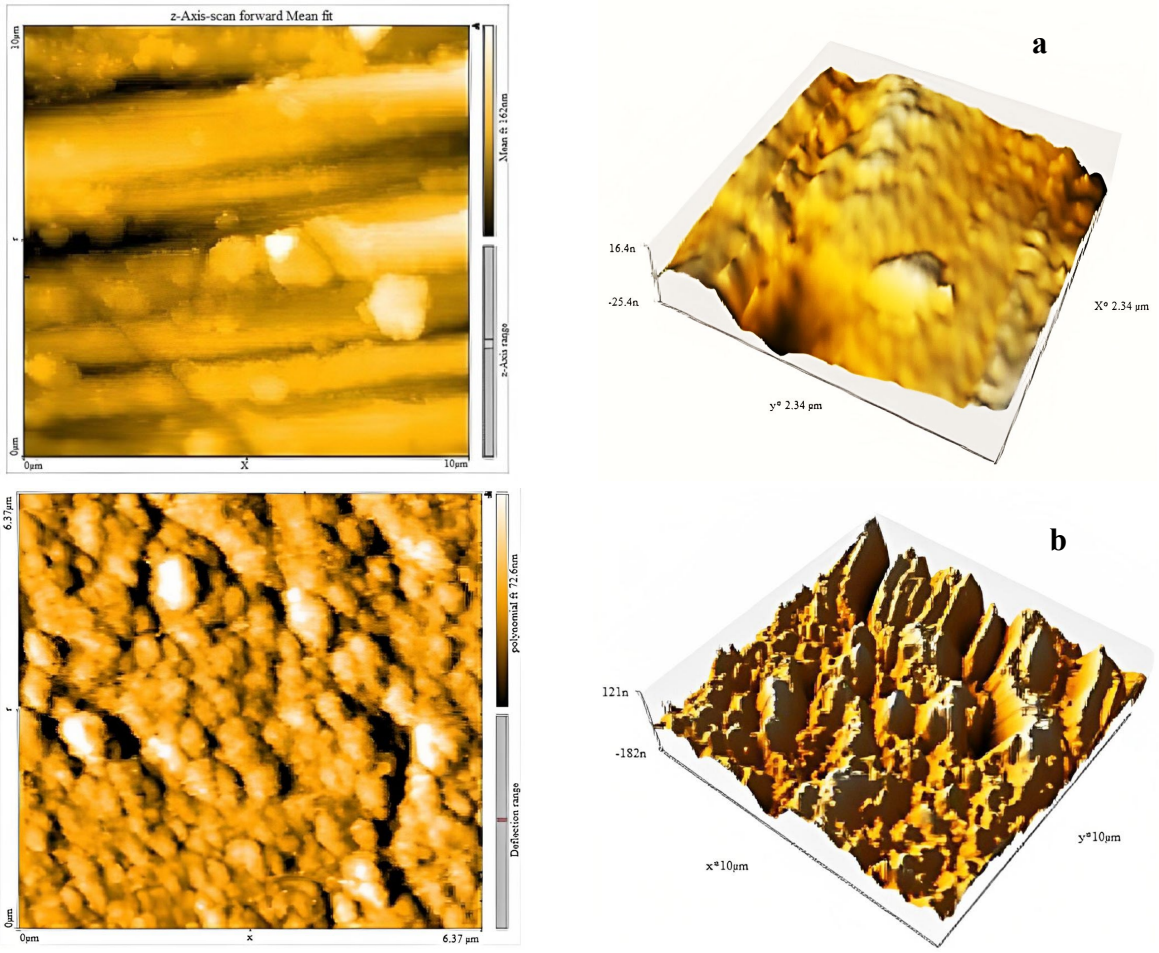

Figure 5: Illustration for AFM images of uncoated (a) and $GdSmTi$ coated (b) $SS\ 316L$

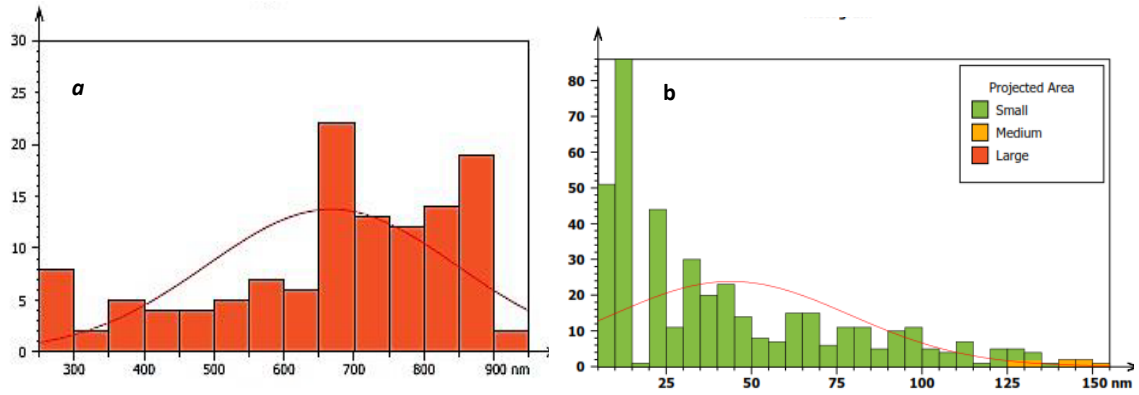

Figure 6: Particle analysis of uncoated (a) and $GdSmTi$ coated $SS\ 316L$ (b)

3.2 Properties of Coated Specimen

3.2.1 Corrosion behavior

In the electrochemical test, it can be seen that the behavior of potential with time gives a clear decrease in the curve followed by stability because of the compatibility with the solution's species, as shown in Figure 7 (a).

For polarization behavior in Figure 7 (b), the decrease in current density is very clear, and the decrease in Tafel slopes is attributed to the reduction of cathodic and anodic sites as well as decreasing in concentration polarization to give very higher resistance and excellent efficiency reached 99.02% due to the role of Gd and its phase with Ni, where it was previously mentioned that the Gd result in a dense coating layer that can give good prevention between the material and the environment. The cyclic polarization in Figure 7 (c), confirms the later result, where there was no appearance of a hysteresis loop in this curve, and then there is a tendency to pitting and after a breakdown at +970 mV, the curve shifted immediately to lower current densities with a wide range of passivity.

The polarization resistance (R_P) was calculated using Tafel slopes (b_c & b_a), Equation (1) which increased from (10.79×10^3) $\Omega.cm^2$ to (703.52×10^3) $\Omega.cm^2$, while protection efficiency ($PE\%$) was estimated using the current density for coated sample ($i_{corr,coated}$) and uncoated sample ($i_{corr,uncoated}$) as follow to give efficiency of 99.02% as listed in Table 3:

$$R_P = \frac{b_c \times b_a}{2.3 \times i_{corr}(b_c + b_a)} \quad (1)$$

$$PE\% = \left[1 - \frac{i_{corr,coated}}{i_{corr,uncoated}}\right] \times 100 \quad (2)$$

Table 3: Corrosion data of uncoated and coated SS 316L by GdSmTi

Sample	$-E_{corr}$, mV	i_{corr}, $\times 10^{-3}$ mA. cm^2	$-b_c$	$+b_a$ V. dec^{-1}	R_P, $\times 10^3$ Ω. cm^2	PE %
Uncoated	243	4.256	0.131	0.549	10.79	
Coated	306	0.0417	0.090	0.271	703.52	99.02

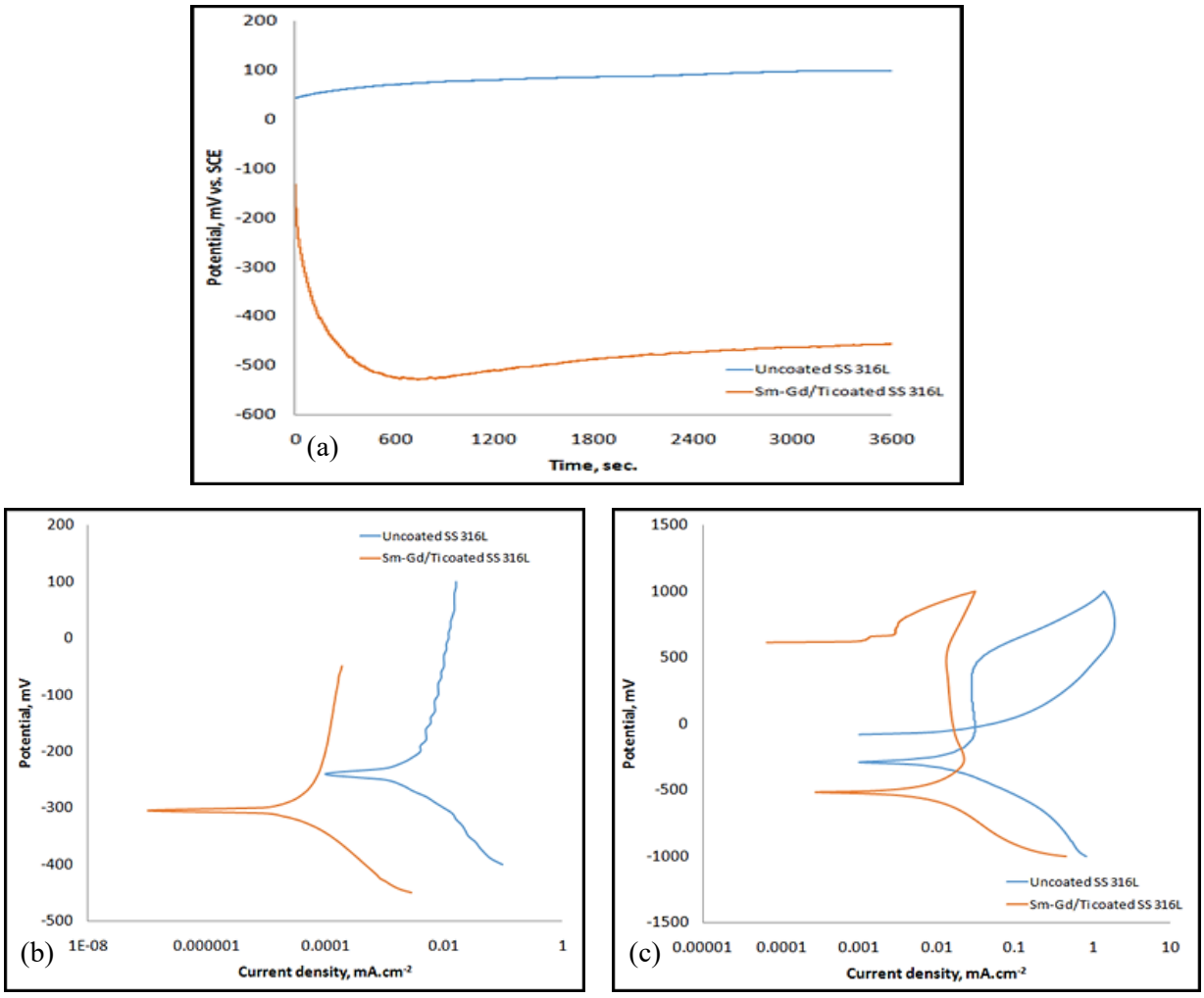

Figure 7: Electrochemical behavior of $GdSmTi$ coated $316L$

3.2.2 Hardness

Hardness is one of the interesting properties that hard films with an increased amount of interfaces can reveal. Uncoated SS 316L had a hardness value of 187 HV, compared to 119 HV for the coated sample. Despite the thin film deposited by the DC sputtering technique from the corresponding target which must have higher hardness due to high residual stress and growth defect hardening and this mechanism introduces a super hardness effect as illustrated by Paul et al. [19], when they deposited TiB_2 layer as nanocolumnar structure by DC sputtering, but in the current work the presence of rare metals decrease the hardness.

3.2.3 Wettability

The measurement of wettability (or contact angle) is related to the hydrophilic and hydrophobic properties of the surface, especially in bio implantation through osteoconductivity. These digital pictures were examined, and the average contact angle was calculated using the tangent method from the right and left angles extracted from images of the drops in equilibrium, as explained by Hassen et al. [20], when determining the drops of three different liquids were measured (formamide, diiodomethane, and water), that deposited on functionalized and bare gold surfaces.

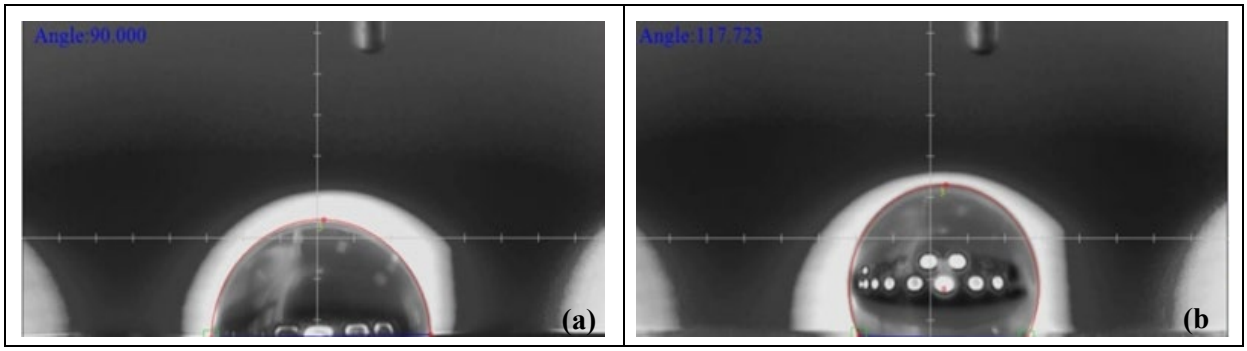

Figure 8: The contact angle of uncoated (a) and coated specimens (b)

The contact angle of the base SS 316L surface is (90°), as shown in Figure 8 (a), while the presence of Gd and Sm led to an increase in the contact angle to (117.723°), as shown in Figure 8 (b), that increases the hydrophilicity, which is in agreement with decreasing of surface roughness, where the wettability is depended mainly on some factors such as the chemical stability of the surface and surface properties

4. Conclusion

Applying GdSm with Ti as a coating to protect stainless steel 316L substrate by DC sputtering technique gave good results in bio application when used as a metallic implant, through the produced dense compact layer on a substrate with various phases clarified by XRD, while SEM/EDS showed the distribution of coating metals with lower roughness from AFM test. The corrosion behavior obtained excellent protection efficiency with increasing the polarization resistance and decreasing current density, as well as some properties achieved, such as decreasing hardness and higher contact angle (wettability); all these results indicate enhancing the osteointegration in implantation.

Author contributions

Conceptualization, H. Jaber, Sh. Naser and R. Anaee; methodology, H. Jaber; Validation, H. Jaber; resources, Sh. Naser; data curation R. Anaee; writing—review and editing, R. Anaee; supervision, H. Jaber and R. Anaee. All authors have read and agreed to the published version of the manuscript.

Funding

This research received no specific grant from any funding agency in the public, commercial, or not-for-profit sectors.

Data availability statement

The data that support the findings of this study are available on request from the corresponding author.

Conflicts of interest

The authors declare that there is no conflict of interest.

References

[1] S. Rafique, M. Idrees, A. Nasim, H. Akbar and A. Athar, Transition metal complexes as potential therapeutic agents, Biotechnol. Mol. Biol. Reviews, 5 (2010) 38–45.

[2] W. B. Jensen, The place of zinc, cadmium, and mercury in periodic table, J. Chem. Educ., 8 (2003) 952–961. https://doi.org/10.1021/ed080p952

[3] A. Cârâc, Biological and biomedical applications of the lanthanides compounds : a mini Review, Proc. Rom. Acad., 19 (2017) 69–74.

[4] S. Sathishkumar, K. Louis, E. Shinyjoy and D. Gopi, Tailoring the Sm/Gd substituted hydroxyapatite coating on biomedical AISI 316L SS: exploration of corrosion resistance, protein profiling, osteocompatibility and osteogenic differentiation for orthopedic implant applications, Ind. Eng. Chem. Res., 10 (2016) 2–49. https://doi.org/10.1021/acs.iecr.5b04329

[5] S. Achache, S. Lamri, M. A. Yazdi, A. Billard, M. François and F. Sanchette, Ni-free super elastic binary Ti–Nb coatings obtained by DC magnetron Co-sputtering, Surf. Coat. Technol., 275 (2015) 283–288. https://doi.org/10.1016/j.surfcoat.2015.05.005

[6] D. Cristea, I. Velicu, L. Cunha, N. Barradas, E. Alves and V. Craciun, Tantalum-titanium oxynitride thin films deposited by DC reactive magnetron Co-Sputtering: mechanical, optical, and tlectrical characterization, Coatings, 12 (2022) 1–16. https://doi.org/10.3390/coatings12010036

[7] Z. Ding, Q. Zhou, Y. Wang, Z. Ding, Y. Tang and Q. He, Microstructure and properties of monolayer, bilayer and multilayer Ta2O5-based coatings on biomedical Ti-6Al-4V alloy by magnetron sputtering, Ceram. Int., 47 (2021) 1133-1144. https://doi.org/10.1016/j.ceramint.2020.08.230

[8] P. Briois, M. A. Yazdi, N. Martin and A. Billard, Pt–Ti alloy coatings deposited by DC magnetron sputtering: A potential current collector at high temperature, Coatings, 10 (2020) 1–10. https://doi.org/10.3390/coatings10030224

[9] M. Mazur, T. Howind, D. Gibson, D. Kaczmarek, Sh. Song, D. Wojcieszak, W. Zhu, P. Mazur, J. Domaradzki and F. Placido, Investigation of structural, optical and micro-mechanical properties of (NdyTi1 − y) Ox thin films deposited by magnetron sputtering, Mater. Des., 85 (2015) 377–388. https://doi.org/10.1016/j.matdes.2015.07.005

[10] S. L. Iconaru, A. Groza, S. Gaiaschi, K. Rokosz, S. Raaen, S. C. Ciobanu, P. Chapon and D. Predoi, Antimicrobial properties of samarium doped hydroxyapatite suspensions and coatings, Coatings, 10 (2020) 1124. https://doi.org/10.3390/coatings10111124

[11] K. Saranya , S. Bhuvaneswari, S. Chatterjee and N. Rajendran, Biocompatible gadolinium-coated magnesium alloy for biomedical applications, J. Mater. Sci., 55 (2020) 11582–11596.

[12] K. Saranya, M. Kalaiyarasan, P. Agilan and *N.* Rajendran, Biofunctionalization of Mg implants with gadolinium coating for bone regeneration, Surf. Interfaces., 31 (2022) 1–13. https://doi.org/10.1016/j.surfin.2022.101948

[13] S. Kannan and R. Nallaiyan, Anticancer activity of samarium-coated magnesium implants for immunocompromised patients, ACS Appl. Bio Mater., 3 (2020) 4408– 4416. https://doi.org/10.1021/acsabm.0c00400

[14] I. C. Nica, M. Popa, L. Marutescu, A. Dinischiotu, S. L. Iconaru, S. C. Ciobanu and D. Predoi, Biocompatibility and antibiofilm properties of samarium doped hydroxyapatite coatings: an in vitro study, Coatings, 11 (2021) 1185. https://doi.org/10.3390/coatings11101185

[15] Kirchmayr, H.R., Burzo E. Landolt-Börnstein-Group III Condensed Matter Numerical Data and Functional Relationships in Science and Technology, Springer-Verlag, Berlin, 1990.

[16] G. Xu , Y.-W. Cui , H. Fei , L. Zhang , F. Zheng , L. Liu and Z. Jin, Phase equilibria in the Gd –Ni binary and Mg –Ni – Gd ternary systems, Int. J. Mater. Res., 103 (2012) 1179–1187. https://doi.org/10.3139/146.110756

[17] D. Padayachee, A. S. Mahomed, S. Singh and H. B. Friedrich, Effect of the TiO2 anatase/rutile ratio and interface for the oxidative activation of n-octane, ACS catal., 10 (2020) 2211–2220. https://doi.org/10.1021/acscatal.9b04004

[18] K. Shalini and S. A. Shivashankar, Oriented growth of thin films of samarium oxide by MOCVD, Bull. Mater. Sci., 28 (2005) 49–54.

[19] P. H. Mayrhofer, H. Clemens and C. Mitterer, Interfaces in nanostructured thin films and their influence on hardness, Int. J. Mater. Res., 96 (2005) 468–480.

[20] H. Touzi, Y. Chevalier, M. Martin, H. B. Ouada and N. J. Renault, Detection of gadolinium with an impedimetric platform based on gold electrodes functionalized by 2-methylpyridine-substituted cyclam, Sensors , 21 (2021) 2–18. https://doi.org/10.3390/s21051658